

## SELF-SIMILAR TEMPERATURE, PRESSURE AND MOISTURE DISTRIBUTIONS WITHIN AN INTENSELY HEATED POROUS HALF SPACE

ABRAHAM DAYAN

Department of Fluid Mechanics and Heat Transfer, Tel-Aviv University, Israel

(Received 5 November 1981)

**Abstract**—A model for the transient heat and mass transfer within an intensely heated porous half space is presented. The model is based on three principal transport phenomena: heat conduction, vapor convection under pressure gradients and the evaporation-recondensation mechanism. Local liquid-vapor equilibrium is assumed. The governing equations consist of two sets: one for the porous region that has dried and one for the remaining moist region. A self-similar solution is obtained for the combination of uniform initial conditions with a step change in boundary conditions. Transient temperature, pressure and moisture distributions are described in closed form for the dry region and numerically for the moist region. The model was applied to study the rate of moisture loss from a drying concrete wall. The results correspond well with results of previously reported investigations.

### NOMENCLATURE

$a$ ,	constant, $1.055 \times 10^{21}$ [atm. K <sup>5</sup> ] for water;
$A$ ,	dimensionless constant, $a/(t_w^5 p_w)$ ;
$b$ ,	constant, 7000[K] for water;
$B$ ,	dimensionless constant, $b/t_w$ ;
$c$ ,	specific heat;
$C$ ,	constant defined after equation (22);
$D$ ,	Darcy's coefficient;
$h_{fg}$ ,	latent heat of vaporization;
$k$ ,	dry region permeability;
$K_d$ ,	dry zone thermal conductivity;
$K_w$ ,	wet zone thermal conductivity;
$\bar{K}$ ,	ratio of the thermal conductivities, $K_w/K_d$ ;
$p$ ,	vapor pressure;
$P$ ,	dimensionless pressure, $p/p_w$ ;
$R_v$ ,	gas constant of vapor;
$S$ ,	volume fraction of pores occupied by vapor;
$t$ ,	absolute temperature;
$T$ ,	dimensionless temperature, $t/t_w$ ;
$u$ ,	velocity;
$x$ ,	distance from heated surface;
$X$ ,	interface location;
$Y_{1,2}$ ,	dimensionless functions defined after equation (23).

$\mu$ ,	viscosity;
$\rho$ ,	density;
$\tau$ ,	time;
$\psi$ ,	dimensionless function defined by equation (14);
$\chi$ ,	dimensionless parameter, $(2\varepsilon \rho_1 h_{fg})/(\rho_s c_s (1 - \varepsilon)t_w)$ .

### Subscripts

$int$ ,	interface;
$l$ ,	liquid;
$0$ ,	initial conditions;
$s$ ,	solid material;
$w$ ,	surface conditions.

### 1. INTRODUCTION

THE WORK presented in this paper is concerned with the thermohydraulic response of a porous structure to intense heating. It was undertaken with the specific purpose of evaluating rates of vapor release from concrete walls in nuclear reactors under accident conditions. In liquid-metal fast breeder reactors, for instance, knowledge of the rate of moisture release from a concrete floor following a sodium spill accident is extremely important. It determines the magnitude of the heat source generated by the chemical reaction between sodium and steam. Application of similar theories has been made before in studies on the drying of clay bricks, pressure generation during sintering processes, pressure generation during the casting of metals in sand molds, damage to buildings following fires, and in other studies.

Early studies on the drying of porous media were mainly concerned with low temperature drying. The models were formulated on the principles of irreversible thermodynamics, first without pressure gradient terms [1-4], and later with those terms [5-7]. In these investigations moisture migration was assumed to take

### Greek symbols

$\alpha$ ,	dry zone thermal diffusivity;
$\bar{\alpha}$ ,	ratio of dry zone to wet zone thermal diffusivities;
$\beta$ ,	dimensionless parameter, $(2\alpha\varepsilon \mu \rho_1 R_v t_w)/(k p_w^2)$ ;
$\gamma$ ,	dimensionless parameter, $(h_{fg} k p_w^2)/(K_w \mu R_v t_w^2)$ ;
$\varepsilon$ ,	porosity;
$\eta$ ,	dimensionless variable, $x/[(4\alpha\tau)^{1/2}]$ ;

place predominantly in the gaseous phase and sorption curves were used to calculate the local equilibrium moisture content. The importance of the evaporation-recondensation mechanism during the pendular stage of drying was pointed out repeatedly. In studies on high temperature drying, indirect modes of transport, such the Soret and Dufour effects, were neglected. Moisture migration was attributed primarily to pressure [8–11] and concentration gradients [12].

Research work on mass transfer in concrete followed a path similar to that of porous media. Moisture transport was first regarded as a process governed by concentration [13] and temperature gradients (Soret effect) [14]. Later, drying experiments at elevated temperatures revealed high pore pressures as a consequence of intense water vaporization [15–17]. For such conditions, vapor filtration under pressure gradients were found to be the primary mode of moisture transfer. Augmented moisture contents, in relatively low temperature areas of the specimens, were also reported. This further supports the evaporation-recondensation theory. The measured pore pressure, determined under equilibrium heating conditions, corresponded well with the sum of the calculated saturated water vapor pressure and ambient air pressure [15].

In recent analyses on high temperature drying of concrete, moisture transport was modeled on the basis of the evaporation-recondensation mechanism with concentration and pressure gradient terms [18–21]. Air transport terms were also included in these analyses. These models were solved numerically and required extensive computation time for accurate predictions. The models were successfully tested with limited experimental data [22]. The purpose of the present work is to propose a simplified version of the above models. It was developed after a careful inspection of the results obtained from previous investigations. The model contains only important transport terms for applications in studies of heat and mass transfer in porous media of low permeability under intense heating conditions.

## 2. PHYSICAL MODEL

The physical model consists of a semi-infinite porous structure heated at the surface. The structure is divided into two regions, one dry, the other wet (Fig. 1). A portion of the heat that penetrates the dry region evaporates water at the dry-wet interface. The other portion enters the wet region by means of thermal conduction. Maximal pore pressures are at the dry-wet interface. Vapor flows from the interface towards both the heated surface and the deeper areas of the structure. Local equilibrium conditions require that vapor must recondense since it has infiltrated the region in a relatively superheated state. This is known as the evaporation-recondensation mechanism, and is responsible for both the enhanced heat transfer and augmented moisture in the wet region.

Previous studies [19, 22] indicated that under intense heating conditions air is evacuated from most of the heated zone. It remains only in a very narrow zone near the heated surfaces, and in deep zones of the structure. The total pressure where air exists is close to the ambient atmospheric pressure. In areas of higher pressure the vapor flow is too intense to allow any inward air diffusion. In view of these facts, it was concluded that the presence of air could affect only boundary conditions and not the field equations of the heated zone. Consequently, the following assumptions were introduced:

- (i) the transport equations include only vapor terms;
- (ii) the vapor flow rate out of the structure would remain unchanged regardless of whether air or vapor, at atmospheric pressure, exists near the heated surface;
- (iii) the existence of air within unheated or slightly heated zones does not affect the overall vapor transport.

Assumption (ii) is equivalent to neglecting mass diffusion within the porous structure near the heated surface. This is justified due to the relatively strong outward vapor flow. Assumption (iii) is based on the fact that the vapor transport rate at the deep edge of the heated zone is determined by temperature gradients rather than viscous forces. In that area the temperature gradients are governed by thermal conduction and cause saturated vapor pressure gradients. The vapor transport rate is negligible due to both small vapor density and weak pressure gradients. The influence of air on the local energy transport or vapor pressure gradients is minimal. Assumption (iii) may not hold in the case of higher than atmospheric ambient air pressures. Under such conditions the existence of air can affect the vapor flow in areas of steep pressure gradients. This requires a different treatment of the boundary condition at the deep edge of the heated zone [23]. Note that the formulation without air is exact for problems involving one component only.

The mathematical model for calculating vapor transport was based on the following assumptions:

- (a) moisture storage is significant only in the liquid phase;
- (b) the thermal conductivity is constant within each zone (but not equal);

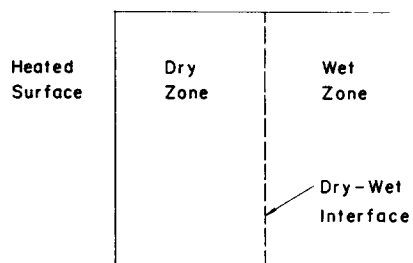


FIG. 1. Physical model of a heated porous structure.

- (c) the specific heat of each zone is constant  $[(1 - \varepsilon)\rho_s c_s + \varepsilon\rho_l c_l(1 - S_0)]$ ;
- (d) the latent heat of vaporization is constant;
- (e) the vapor velocity obeys Darcy's law with a moisture dependent coefficient,  $u = -D \frac{\partial p}{\partial x}$ ;
- (f) Darcy's coefficient is linearly dependent on  $S$ ,  $D = (k/\mu)S$ ;
- (g) liquid mobility is negligible especially in concrete in view of the fine size of the gel pores (20 Å) and their enormous specific surface, ( $2 \times 10^6 \text{ cm}^2 \text{ g}^{-1}$ ) [13];
- (h) vapor behaves as an ideal gas,  $p = \rho_v R_v t$ ;
- (i) the vapor is in equilibrium with the liquid phase in the wet region,  $p = a t^{-5} \exp(-b/t)$ ;
- (j) the convection of sensible heat in the vapor phase is negligible;
- (k) the temperature of the dry-wet interface is constant and depends on both initial and boundary conditions (this implies that the moisture content at the interface remains unchanged during the drying process).

The conservation equations for mass and energy transport in the dry region are, respectively,

$$\frac{\partial}{\partial x}(u\rho_v) = 0 \quad (1)$$

and

$$(1 - \varepsilon)\rho_s c_s \frac{\partial t}{\partial \tau} = K_d \frac{\partial^2 t}{\partial x^2}. \quad (2)$$

Equation (1) states that moisture cannot be stored in the dry region. The continuity and energy equations of the wet region are, respectively,

$$\varepsilon\rho_l \frac{\partial S}{\partial \tau} = \frac{\partial}{\partial x}(u\rho_v), \quad (3)$$

and

$$[(1 - \varepsilon)\rho_s c_s + \varepsilon\rho_l c_l(1 - S_0)] \frac{\partial t}{\partial \tau} + \varepsilon\rho_l h_{fg} \frac{\partial S}{\partial \tau} = K_w \frac{\partial^2 t}{\partial x^2}. \quad (4)$$

Equation (3) indicates that phase change is the source or sink of vapor. Equation (4) contains a source term which means that energy is delivered into the wet region by recondensation of vapor.

In addition to the above equations, the following continuity conditions must exist at the interface:

$$(u\rho_v)_{\text{int}+} - (u\rho_v)_{\text{int}-} = \varepsilon\rho_l \left[ (1 - S) \frac{dX}{d\tau} \right]_{\text{int}}, \quad (5)$$

$$K_w \left( \frac{\partial t}{\partial x} \right)_{\text{int}+} - K_d \left( \frac{\partial t}{\partial x} \right)_{\text{int}-} = \varepsilon\rho_l h_{fg} \left[ (1 - S) \frac{dX}{d\tau} \right]_{\text{int}}. \quad (6)$$

Equation (5) states that the vapor mass flow rate from the interface equals the rate of moisture vaporization.

Equation (6) shows that the difference between the heat flow that reaches the interface and the heat that enters the wet region is consumed by vaporization and displacement of the interface.

In the present analysis the governing equations were subjected to uniform initial conditions,

$$S(x, 0) = S_0, \quad (7)$$

$$t(x, 0) = t_0$$

and boundary conditions of constant ambient pressure with a step change in surface temperature

$$P(0, \tau) = P_0 = P_w, \quad (8)$$

$$t(0, \tau) = t_w.$$

For the above initial and boundary conditions the governing equations can be transformed to ordinary differential equations with a similarity variable

$$\eta = x/(4\alpha\tau)^{1/2}. \quad (9)$$

The dimensionless forms of the equations are

$$\frac{d}{d\eta} \left( \frac{1}{T} \frac{dP^2}{d\eta} \right) = 0 \quad (10)$$

and

$$\frac{d^2 T}{d\eta^2} + 2\eta \frac{dT}{d\eta} = 0 \quad (11)$$

for the dry region, and for the wet region

$$\frac{d}{d\eta} \left( S\psi \frac{dT}{d\eta} \right) - \beta\eta \frac{dS}{d\eta} = 0 \quad (12)$$

and

$$\frac{d^2 T}{d\eta^2} + 2\bar{\alpha}\eta \frac{dT}{d\eta} + \gamma\beta\eta \frac{dS}{d\eta} = 0. \quad (13)$$

The function  $\psi$  is temperature dependent and arises from the conversion of pressure derivatives to temperature derivatives following  $dP/d\eta = (dP/dT)dT/d\eta$ . The term in the bracket is simply the temperature derivative of the saturation pressure [see assumption (i)]. The function  $\psi$  is defined by

$$\psi = \frac{A^2}{T^{12}} \left( \frac{B}{T} - 5 \right) \exp \left( -\frac{2B}{T} \right). \quad (14)$$

The dimensionless forms of the continuity conditions at the dry-wet interface are

$$\left( \frac{dP}{d\eta} \right)_{\text{int}-} - \left( S \frac{dP}{dT} \frac{dT}{d\eta} \right)_{\text{int}+} = \left[ \beta \left( \frac{T}{P} \right) \eta (1 - S) \right]_{\text{int}} \quad (15)$$

and

$$\left( -\frac{dT}{d\eta} \right)_{\text{int}-} + \bar{K} \left( \frac{dT}{d\eta} \right)_{\text{int}+} = [\chi\eta(1 - S)]_{\text{int}}. \quad (16)$$

Note that a similarity solution requires that  $X = \eta_{\text{int}}(4\alpha\tau)^{1/2}$  ( $\eta_{\text{int}}$  stands as a proportionality constant).

The dimensionless representations of the initial and boundary conditions are, respectively,

$$S(\eta = \infty) = S_0, \tag{17}$$

$$T(\eta = \infty) = T_0 \tag{18}$$

and

$$P(\eta = 0) = 1, \tag{19}$$

$$T(\eta = 0) = 1. \tag{20}$$

3. SOLUTION

The temperature and pressure distributions of the dry region are obtained from a direct integration of equations (11) and (10), respectively,

$$T = 1 - (1 - T_{int}) \frac{\text{erf}(\eta)}{\text{erf}(\eta_{int})} \tag{21}$$

and

$$P^2 = 1 + C \left\{ \left[ 1 - \frac{1 - T_{int}}{\text{erf}(\eta_{int})} \right] \eta + \frac{1 - T_{int}}{\text{erf}(\eta_{int})} \left[ \eta \text{erfc}(\eta) + \left( \frac{1}{\pi^{1/2}} \right) [1 - \exp(-\eta^2)] \right] \right\}. \tag{22}$$

Both expressions are dependent on the interface location  $\eta_{int}$  and temperature  $T_{int}$ . These two parameters are, in turn, dependent on the initial and boundary conditions. Their values, like most of Stefan's problem, cannot be expressed in closed form. Here they are found by an iteration process. For each selection of  $\eta_{int}$  and  $T_{int}$  the equations of the wet zone are integrated numerically. The correct selection of  $\eta_{int}$  and  $T_{int}$  should give a solution which asymptotically satisfies the initial conditions as  $\eta \rightarrow \infty$ . The constant of integration  $C$ , in equation (22), depends only on  $\eta_{int}$  and  $T_{int}$ . The equation can be readily solved for  $C$  following the substitution of the saturation pressure  $P(T_{int})$  [see assumption (i)].

In order to proceed with the solution of the wet region, consider the interface conditions, equations (15) and (16). They contain two unknowns: the saturation parameter at the interface, and the temperature derivative to the right of the interface. The solution of these equations is

$$S_{int} = [-Y_1 + (Y_1^2 - 4Y_2)^{1/2}]/2 \tag{23}$$

and

$$\left( \frac{dT}{d\eta} \right)_{int+} = \left[ \chi \eta_{int} (1 - S_{int}) + \left( \frac{dT}{d\eta} \right)_{int-} \right] / \bar{K} \tag{24}$$

where

$$Y_1 = \frac{\beta \bar{K} \left( \eta \frac{T}{P} \right)_{int} - \left[ \chi \eta_{int} + \left( \frac{dT}{d\eta} \right)_{int-} \right] \left( \frac{dP}{dT} \right)_{int}}{\chi \eta_{int} \left( \frac{dP}{dT} \right)_{int}}$$

$$Y_2 \equiv \bar{K} \frac{\left( \frac{dP}{d\eta} \right)_{int-} - \beta \left( \eta \frac{T}{P} \right)_{int}}{\chi \eta_{int} \left( \frac{dP}{dT} \right)_{int}}$$

and

$$\left( \frac{dP}{dT} \right)_{int} = (B - 5 T_{int}) \left( \frac{P}{T^2} \right)_{int}, \tag{25}$$

$$\left( \frac{dT}{d\eta} \right)_{int-} = (T_{int} - 1) \left[ \frac{2 \exp(-\eta_{int}^2)}{\pi^{1/2} \text{erf}(\eta_{int})} \right], \tag{26}$$

$$\left( \frac{dP}{d\eta} \right)_{int-} = \frac{C}{2} \left( \frac{T}{P} \right)_{int}. \tag{27}$$

The saturation parameter  $S_{int}$  was obtained from the solution of a quadratic equation. The second root of the equation does not satisfy the requirement  $0 \leq S \leq 1$  and thus is inapplicable.

Two boundary conditions are required for the solution of the temperature field in the wet region. Only one boundary condition is necessary for the solution of the vapor saturation parameter  $S$ . Equations (23) and (24) are two of these conditions at  $\eta_{int}$ .  $T_{int}$  is the third necessary condition. The selection of  $\eta_{int}$  and  $T_{int}$  as boundary conditions may seem less appropriate than a selection of boundary conditions at infinity, namely  $S_0$  and  $T_0$ . In practice it makes no difference where the conditions are specified. By using an iteration procedure one can find the correspondence between different sets of boundary conditions.

The moisture and temperature distributions of the wet region were obtained numerically. Before integration, equations (12) and (13) were solved for the saturation-parameter derivative

$$\frac{dS}{d\eta} = \frac{\left[ \left( \frac{(2B - 15T)(B - 4T)}{T^2(B - 5T)} \right) \frac{dT}{d\eta} \right] - 2\bar{\alpha}\eta}{\left[ \left( \frac{1}{\psi} + \gamma S \right) \beta \eta - \frac{dT}{d\eta} \right]} S \frac{dT}{d\eta}. \tag{28}$$

Equations (28) and (13) were integrated numerically using a Runge-Kutta routine. The integration procedure began by a systematic selection of  $\eta_{int}$  and  $T_{int}$ . Equations (23) and (24) were used to calculate  $S_{int}$  and  $(dT/d\eta)_{int}$ . Beginning at  $\eta_{int}$  the integration proceeded towards  $\eta \rightarrow \infty$ . Based on known values of  $S$ ,  $T$  and  $dT/d\eta$ , at a given  $\eta$ , new values were computed at  $\eta + \Delta\eta$ . New values of  $S$  were computed with equation (28), and new temperature derivatives with equation (13). At large  $\eta$  (about  $\eta = 4$ ) the temperature  $T$  and saturation parameter  $S$  assumed almost constant values. These were compared to the initial conditions to determine when a new selection of interface conditions was required. For parametric studies, however, such iterations are not required. For given boundary conditions, variations of  $\eta_{int}$  and  $T_{int}$  are equivalent to variations of initial conditions,  $T_0$  and  $S_0$ .

Table 1. Values of dimensionless parameters used in the analysis

	$A$	$B$	$\bar{K}$	$1-S_0$	$T_0$	$\bar{\alpha}$	$\beta$	$\gamma$	$\chi$
N1	$1.124 \times 10^7$	11.24	1.5	0.055	0.48	0.693	176.7	$4.72 \times 10^{-3}$	1.252
N2	$1.124 \times 10^7$	11.24	1.5	0.131	0.48	0.728	176.7	$4.72 \times 10^{-3}$	1.252
N3	$1.124 \times 10^7$	11.24	1.5	0.296	0.48	0.797	176.7	$4.72 \times 10^{-3}$	1.252
N4	$1.124 \times 10^7$	11.24	1.5	0.690	0.48	0.967	176.7	$4.72 \times 10^{-3}$	1.252
N5	$2.696 \times 10^7$	13.38	1.5	0.873	0.57	1.047	148.4	$6.70 \times 10^{-3}$	1.492
N6	$1.708 \times 10^7$	12.22	1.5	0.441	0.52	0.857	162.5	$5.59 \times 10^{-3}$	1.362
N7	$1.708 \times 10^7$	12.22	1.5	0.073	0.52	0.698	812.6	$1.12 \times 10^{-3}$	1.362

#### 4. RESULTS AND DISCUSSION

Transient temperature, pressure and moisture distributions were calculated for material properties typical to those of concrete. The corresponding dimensionless parameters used in the analysis are summarized in Table 1. The results obtained are for porous media which are initially in equilibrium with a standard atmosphere (1 atm., 25°C). All the transient distributions presented are for the boundary conditions of a step change in wall temperature.

Characteristic temperature distributions are shown in Fig. 2. The discontinuity in the slope of the temperature profiles designates the location of the dry-wet interface. Reduced temperature gradients in the wet region, as compared to the dry region, result from the better thermal conductivity and enhanced heat transfer by the evaporation-recondensation mechanism. This is especially apparent near the interface where moisture recondensation is substantial (Fig. 3). The augmented moisture content, as shown in Fig. 3, results from recondensation. A higher moisture content tends to keep the dry-wet interface closer to the heated surface. Consequently, the interface temperature and pressure are greater (Fig. 4). In contrast, the larger amount of heat required for vaporization inhibits the rate of temperature rise in the heated zone.

Effects of initial moisture content are minimal at points deep in the wet zone.

Inspection of Figs. 3 and 4 reveals that moisture recondensation is pronounced at moderate degrees of saturation. At a large initial moisture content the vapor flow is limited by reduced apparent permeability. At low initial moisture contents pressure gradients become weak and cannot drive an intensive vapor flow. The average rate of moisture loss from a heated structure is expected to increase with the initial amount of moisture owing to greater pressure gradients and smaller sensible heat storage.

From a standpoint of material strength, it is necessary to limit peak pore pressures. This is particularly important in concrete which has a weak tensile strength. In general, higher wall temperatures would produce higher pressures. In order to maintain peak pressures at a constant level one would have to offset effects of higher wall temperatures by selecting drier structures. This is depicted by observing curves N5 and N6 in Figs. 5-7. Comparison of curves N4 and N6 confirms the intuitive fact that higher wall temperatures promote rapid drying rates. Curves N6 and N7 are transient distributions with equal wall temperatures and peak pressures. However, they belong to porous structures of different permeability and initial

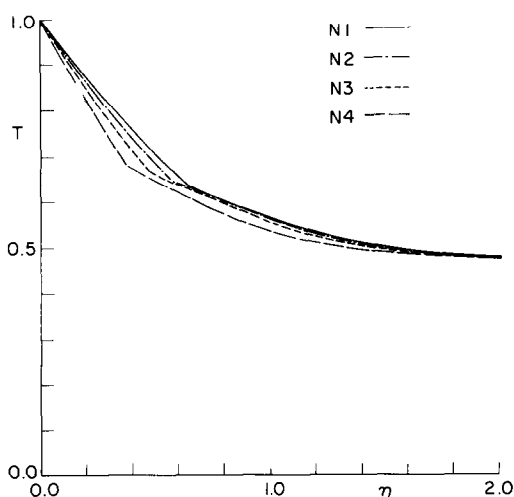


FIG. 2. Temperature distributions within heated porous structures.

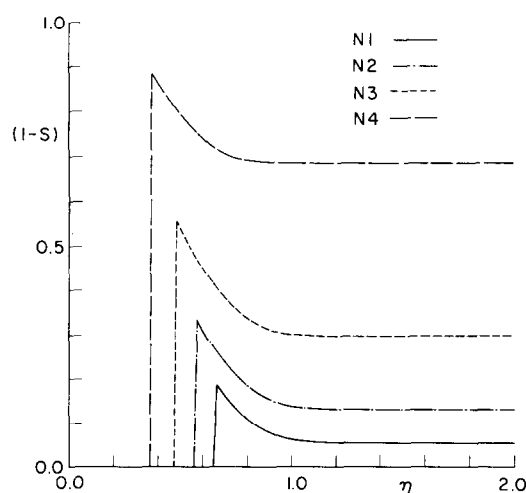


FIG. 3. Moisture distributions within heated porous structures.

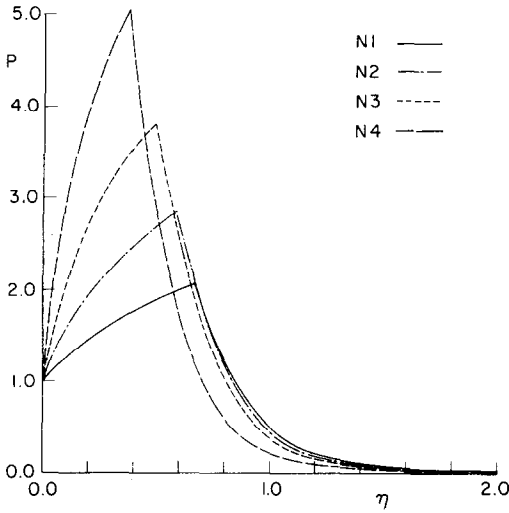


FIG. 4. Pressure distributions within heated porous structures.

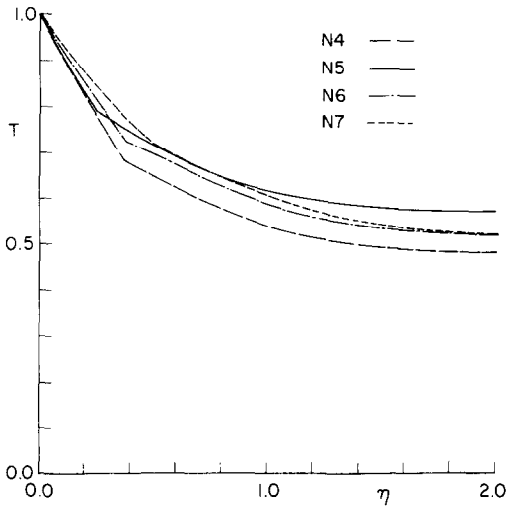


FIG. 5. Temperature distributions within heated porous structures.

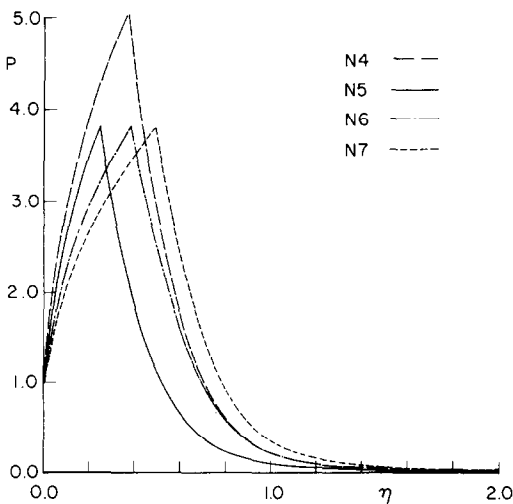


FIG. 6. Pressure distributions within heated porous structures.

moisture content. It is apparent that low permeabilities tend to elevate peak pressures. The increased resistance to vapor flow suppresses the evaporation-recondensation mechanism. Therefore the area of augmented moisture is narrowed and temperature gradients are increased (Figs. 5 and 7).

The worst possible combination that may jeopardize the structural integrity of a porous media is that of high wall temperature, large moisture content and low permeability. In concrete structures pore pressures can reach levels of several atmospheres and cause spallation [21].

Results of the present model were compared with results of the model described previously [22]. The latter, as mentioned earlier, contains terms for the conservation and transport of air including mass diffusion. The parameters used for the calculation of curves N6 were chosen for the comparison. The results showed that the model without terms for air yields a dry zone temperature distribution which is less than 3% lower, and a wet zone temperature distribution which becomes 10% higher towards the edge of the heated region. The moisture distribution in the recondensation zone is somewhat higher as required for the higher local temperatures. A negligible difference between the vapor and total pressure at the interface were found in the results of the complete model.

In conclusion it is seen that the present model is a simple and reasonably accurate tool for the prediction of moisture and temperature distributions within intensely heated porous media of low permeability. The fact that the equations were written for one gaseous species does not restrict its applicability to other problems. It can be applied, for instance, to transport calculations in porous media that contain air and vapor provided that the pressure of the former is not too high.

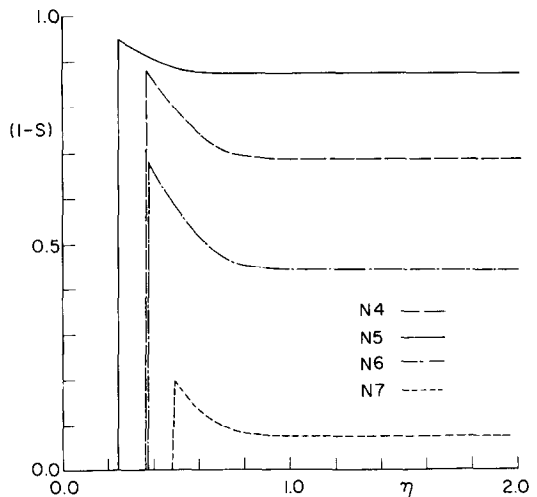


FIG. 7. Moisture distributions within heated porous structures.

## REFERENCES

1. L. N. Gupta, An approximate solution of the generalized Stefan's problem in a porous medium, *Int. J. Heat Mass Transfer* **17**, 313–321 (1974).
2. S. H. Cho, An exact solution of the coupled phase change problem in a porous medium, *Int. J. Heat Mass Transfer* **18**, 1139–1142 (1975).
3. M. D. Michailov and B. K. Shishedjiev, Temperature and moisture distributions during contact drying of moist porous sheet, *Int. J. Heat Mass Transfer* **18**, 15–24 (1975).
4. M. D. Mikhailov, Exact solution of temperature and moisture distributions in a porous half-space with moving evaporation front, *Int. J. Heat Mass Transfer* **18**, 797–804 (1975).
5. T. Z. Harmathy, Simultaneous moisture and heat transfer in porous systems with particular reference to drying, *I/EC Fundamentals* **8**, 92–103 (1969).
6. C. L. D. Huang, H. H. Siang and C. H. Best, Heat and moisture transfer in concrete slab, *Int. J. Heat Mass Transfer* **22**, 252–266 (1979).
7. C. L. D. Huang, Multi-phase moisture transfer in porous media subjected to temperature gradient, *Int. J. Heat Mass Transfer* **22**, 1295–1307 (1979).
8. M. Cross, R. D. Gibson and R. W. Young, Pressure generation during the drying of a porous half-space, *Int. J. Heat Mass Transfer* **22**, 47–50 (1979).
9. R. D. Gibson, M. Cross and R. W. Young, Pressure gradients generated during the drying of porous shapes, *Int. J. Heat Mass Transfer* **22**, 827–830 (1979).
10. F. A. Morrison, Transient multiphase multicomponent flow in porous media, *Int. J. Heat Mass Transfer* **16**, 2331–2342 (1973).
11. H. Saito and N. Seki, Mass transfer and pressure rise in moist porous material subjected to sudden heating, *Trans. Am. Soc. Mech. Engrs, Series C, J. Heat Transfer* **99**, 105–112 (1977).
12. K. Min and H. W. Emmons, The drying of porous media in, *Proc. 1972 Heat Transfer and Fluid Mech. Inst.*, pp. 1–18. Stanford University Press (1972).
13. R. L. Yuan, H. K. Hilsdorf and C. E. Kesler, The effect of temperature on the drying of concrete, in *Concrete for Nuclear Reactors*, Vol. 2, American Concrete Institute Spec. Publ. No. 34, pp. 991–1019 (1972).
14. S. E. Pihlajavara and K. Tinsanen, A preliminary study of thermal moisture transfer in concrete, in *Concrete for Nuclear Reactors*, Vol. 2, American Concrete Institute Spec. Publ. No. 34, pp. 1019–1033 (1972).
15. G. L. England and T. J. Sharp, Migration of moisture and pore pressures in heated concrete, *Proc. 1st Int. Conf. on Structural Mechanics in Reactor Technol.*, H2/4, pp. 129–143 (1971).
16. D. A. Chapman and G. L. England, Effects of moisture migration on shrinkage, pore pressure and other concrete properties, *Trans. 4th Int. Conf. on Structural Mechanics in Reactor Technol.*, H1/3, 1–14 (1977).
17. Z. P. Bazant, Some questions of material inelasticity and failure in the design of concrete structures for nuclear reactors, *Trans. 3rd Int. Conf. on Structural Mechanics in Reactor Technol.*, H1/1\*, pp. 1–11 (1977).
18. M. S. Sahota and P. J. Pagni, Heat and mass transfer in porous media subject to fires, *Int. J. Heat Mass Transfer* **22**, 1069–1081 (1979).
19. E. L. Glueckler and A. Dayan, Considerations of the third line of assurance, post-accident heat removal and core retention in containment, *Proc. Int. Meeting on Fast Reactor Safety and Related Physics*, USERDA Publication, CONF-761001, 4, pp. 1995–2004 (1976).
20. A. Dayan and E. L. Glueckler, Heat and mass transfer behind a heated reactor cell liner, *Trans. Am. Nucl. Soc.* **26**, 401–402 (1977).
21. E. L. Glueckler, A. Dayan, F. Hayes and C. T. Kline, Transient containment response and inherent retention capability, *Int. J. Nucl. Engng Des.* **42**, 151–167 (1977).
22. A. Dayan and E. L. Glueckler, Heat and mass transfer within an intensely heated concrete slab, *Int. J. Heat Mass Transfer* **25**, 1469–1475 (1982).
23. A. Dayan and E. L. Glueckler, Heat and mass transfer during the drying of a concrete structure, To appear in the *Proc. 6th Int. Conf. on Structural Mechanics in Reactor Technol.*, H1/7 (1981).

## DISTRIBUTIONS DE TEMPERATURE DE PRESSION ET D'HUMIDITE DANS UN DEMI-ESPACE POREUX CHAUFFE INTENSEMENT

**Résumé**—On présente un modèle pour le transfert thermique et massique dans un milieu poreux semi-infini et chauffé intensément. Il est basé sur les trois phénomènes principaux : Conduction de la chaleur, convection de la vapeur sous l'effet des gradients de pression et évaporation–recondensation. On suppose l'équilibre liquide–vapeur. Les équations concernent deux systèmes : l'un pour la région poreuse qui a séché et l'autre pour la région encore humide. On obtient une solution affine pour la combinaison des conditions initiales uniformes avec un changement en échelon dans les conditions aux limites. Les distributions variables de température, pression et humidité sont décrites de façon analytique pour la région sèche et numériquement pour la région humide. Le modèle est appliqué à l'étude de la vitesse de séchage pour un mur de béton. Les résultats correspondent bien à ceux antérieurement publiés.

## EINE ÄHNLICHKEITSLÖSUNG FÜR DIE VERTEILUNG VON TEMPERATUR, DRUCK UND FEUCHTIGKEIT IN EINEM STARK BEHEIZTEN PORÖSEN HALBRAUM

**Zusammenfassung**—Es wird ein Modell für den instationären Wärme- und Stofftransport in einem stark beheizten porösen Halbraum vorgestellt. Das Modell beruht auf drei grundlegenden Transportvorgängen : der Wärmeleitung, der Konvektion des Dampfes unter dem Einfluß von Druckgradienten und dem Verdampfungs-Rekondensationsmechanismus. Es wird örtliches Gleichgewicht zwischen Flüssigkeit und Dampf angenommen. Die das Problem beschreibenden Gleichungen bestehen aus zwei Sätzen : einem für das getrocknete poröse Gebiet und einem für das verbleibende feuchte Gebiet. Eine Ähnlichkeitslösung wird erhalten für die Kombination gleichförmiger Anfangsbedingungen mit einer sprungförmigen Änderung der Randbedingungen. Instationäre Temperatur-, Druck- und Feuchtigkeitsverteilungen werden in geschlossener Form für das trockene Gebiet und für das feuchte Gebiet in numerischer Form beschrieben. Das Modell wurde zur Bestimmung des Feuchtigkeitsverluststroms einer trocknenden Betonwand verwendet. Die Ergebnisse stimmen gut mit früher veröffentlichten Untersuchungen überein.

**АВТОМОДЕЛЬНЫЕ РАСПРЕДЕЛЕНИЯ ТЕМПЕРАТУРЫ, ДАВЛЕНИЯ И ВЛАЖНОСТИ  
В ИНТЕНСИВНО НАГРЕВАЕМОМ ПОРИСТОМ ПОЛУПРОСТРАНСТВЕ**

**Аннотация** — Представлена модель нестационарного тепло- и массопереноса в интенсивно нагреваемом полуограниченном пористом теле. В основу модели положены три основные явления переноса: теплопередача, конвекция пара под действием градиентов давления и механизм испарения-переконденсации. Предполагается локальное равновесие между жидкостью и паром. Основные уравнения представлены двумя системами: одна для пористой сухой области и вторая для влажной. Получено автомоделное решение для случая, когда однородные начальные условия сочетаются со ступенчатым изменением граничных условий. Нестационарные профили температуры, давления и влажности описываются аналитически для сухой области и численно для влажной. Модель используется для расчета скорости потери влаги при сушке бетонной плиты. Результаты хорошо согласуются с данными ранее опубликованных исследований.